# Large electric-potential bias in an EDO-TTF tetramer as a major mechanism of charge ordering observed in its $PF_6$ salt: A density functional theory study

Kaoru Iwano[1] and Yukihiro Shimoi[2,3]

[1]*Institute of Materials Structure Science, Graduate University for Advanced Studies, High Energy Accelerator Research Organization (KEK), 1-1 Oho, Tsukuba 305-0801, Japan*

[2]*Nanotechnology Research Institute (NRI), National Institute of Advanced Industrial Science and Technology (AIST), 1-1-1 Umezono, Tsukuba 305-8568, Japan*

[3]*National Institute for Nanotechnology, National Research Council of Canada, 11421 Saskatchewan Drive, Edmonton, Alberta, Canada T6G 2M9*

(Received 5 September 2007; revised manuscript received 28 October 2007; published 20 February 2008)

Based on density functional theory, we investigate the electronic structures of an organic molecular solid, $(EDO\text{-}TTF)_2PF_6$ (EDO-TTF=ethylendioxy-tetrathiafulvalene), which is known to have a so-called charge-ordered state below a critical temperature. While it has been thought that the origins of the charge ordering are molecular deformations, we find that an electric potential bias within a tetramer of EDO-TTF molecules is close to 1 eV, originating from long-range Coulombic interactions with surrounding molecules, and that it is essential in reproducing the actual degree of charge ordering. We also calculate optical conductivity spectra and find a good consistency with experimental results.

DOI: 10.1103/PhysRevB.77.075120 PACS number(s): 71.30.+h, 71.15.Mb, 78.20.Bh

## I. INTRODUCTION

Molecular-based charge-transfer salts provide various solid-state phases and physics due to interplay among electron-correlation, electron-lattice (or -phonon), and disorder effects. Among such phases, the states of charge ordering have been an important issue, since it is deeply related to their basic electronic parameters when it is expressed by a simple extended Hubbard model.[1] When a conduction band is just one-quarter (three-quarter) filled in quasi-one-dimensional systems, we have, roughly speaking, two types of ordering such as 0101 and 0110, with 0 and 1 being the occupancies of outermost electrons (holes) at each site. It is well known that the nearest-neighboring electronic repulsion (so-called $V$) prefers the former pattern.[1]

$(EDO\text{-}TTF)_2X$ ($X$=$PF_6$ and $AsF_6$) quasi-one-dimensional salts with a (3/4)-filled band show the other type of ordering, i.e., 0110, in their low-temperature insulator phase.[2] (See the left picture of Fig. 1.) When we consider its mechanism, it is important that this charge ordering is accompanied by molecular deformations. The most conspicuous one is the intra-molecular deformation that is specified as "Bent" or "Flat" in Fig. 1. Since quantum chemical calculations reveal that an isolated neutral (positively charged) molecule takes a bent (flat) form,[3] valency patterns as shown in Fig. 1 are strongly suggested. In addition, we notice tetramerization along the one-dimensional axis, which is in contrast to the structure of a metal phase above the critical temperature of 278 K.

Very recently, a photoinduced phase transition (PIPT) with ultrafast response was discovered for its $PF_6$ salt by Chollet *et al.*,[4] suggesting the melting of charge ordering and metallization as its result. Such drastic response to light excitations suggests the possible potential of this class of materials for future optical communication. After this work, intensive investigations pursued by the same group revealed that, among the lowest two main peaks in the optical conductivity spectra, an excitation to the higher charge-transfer peak (CT2) drives the PIPT more effectively than the lower one (CT1).[5] Although a complete analysis of their measurements has not been finished yet, this urges our clear understanding of optically excited states as well as the ground state.

In this work, we investigate basic electronic and optical properties of the charge-ordering state of $(EDO\text{-}TTF)_2PF_6$ by applying density functional theory (DFT) calculations to clusters consisting of EDO-TTF molecules. For the ground state, the effects of electron correlation are treated within the hybrid gradient-corrected correlation functional, B3LYP, which we use throughout this study. Meanwhile, for optically excited states, a time-dependent DFT (TD-DFT) method[6] is applied, which can include the effects of the so-called random-phase approximation (RPA) and reproduce the spectra of many molecules successfully, particularly with the choice of B3LYP.[7] Moreover, here we use localized Gaussian basis sets. This is because the Gaussian basis sets are considered to be more effective than plane-wave ones for describing the nature of molecular materials. We demonstrate that a large potential bias within a tetramer, which is caused

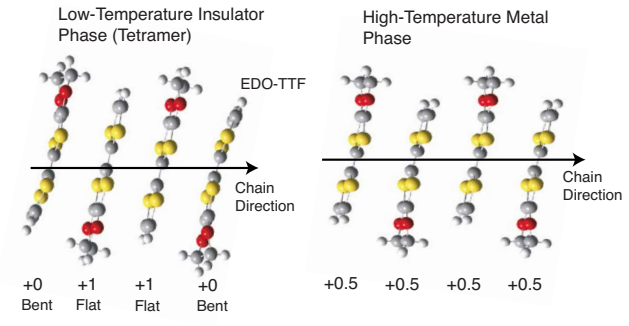


FIG. 1. (Color online) EDO-TTF molecular structures in the two phases.

 

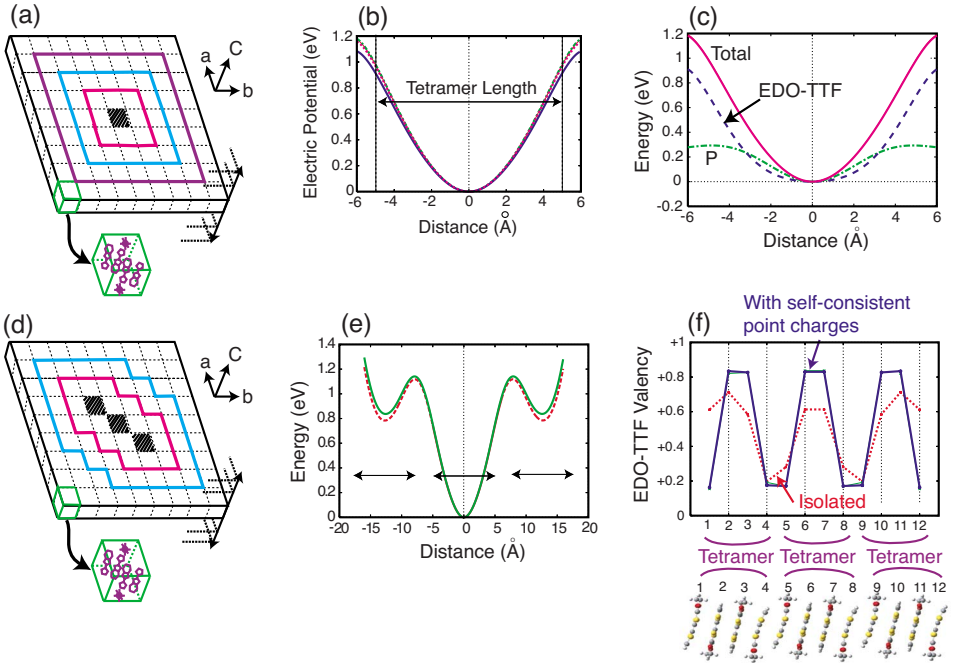


FIG. 2. (Color online) [(a) and (d)] How to increase shells around the system cluster consisting of one tetramer or three tetramers. [(b) and (e)] Electric potentials from the self-consistent point charges surrounding one tetramer and three tetramers, respectively. The direction of the abscissa is along the chain. In both, one-tetramer regions are specified by the horizontal arrows. (c) The components within the potential for one tetramer. (f) Valency patterns of EDO-TTF molecules for the three-tetramer cases.

by electrostatic potentials due to surrounding molecules, is an essential factor to stabilize the charge-ordering state.

We also estimate fundamental electronic parameters such as intermolecular transfer energies and site potentials, and assign transition natures to the optical absorptions peaks, which provide useful basic information to understand the mechanism of PIPT. Regarding the materials, our results on the $PF_6$ salt will be effective semiquantitatively also for the $AsF_6$ salt, since they have very similar electronic and structural properties.[2]

## II. SELF-CONSISTENT TREATMENT OF ENVIRONMENTAL POINT CHARGES

Throughout this study, we utilize the package of GAUSSIAN 03.[8] The basis set is typically that of 6-31G($d$), if not mentioned specially. Instead of a periodic boundary condition, which is very time-consuming when applied to this package, we assume a cluster of one tetramer of EDO-TTF molecules (4 molecules) and that of three tetramers (12 molecules). The tetramer is spatially the most localized unit in this crystal, and is considered to be the most appropriate choice. The validity will be checked by the final result shown later. Regarding the geometrical configuration of the clusters, we use the atomic positions determined by x-ray diffraction.

As shown below, Coulombic interactions arising from a surrounding environment are indispensable to give a realistic description of the electronic structure of this salt. This feature appears most keenly in the degree of charge transfer. First of all, we will introduce our approach that incorporates the effects of the environment as naturally as possible. We place point charges at the atomic positions outside the cluster and let their magnitudes coincide with the valencies of the corresponding atoms within the cluster. The valencies are determined by the natural population analysis[9] and, in the case of a cluster of three tetramers, they are averaged among the three equivalent atoms. We have sought for self-consistency between the point charges and the valencies by iterations, and found that iterations of several times are sufficient. Coulombic interactions arising from charge distribution within the cluster are automatically taken into account in the DFT calculations. Hence, this self-consistent scheme mostly excludes the influence of the choice of the cluster, excepting the termination of itineracy beyond the cluster boundary. As for the anion, recent NMR measurements observed that the molecule is rotating uniaxially under the critical temperature and that an appreciable amount of exchange between the atoms on the axis and the rotating ones exists.[10] Considering this and possible smearing out by electron clouds, we replace all the $PF_6$ molecules with point charges of $-|e|$ located at each P atom for both the ones within a cluster and the ones in the environment.

Since the DFT calculations are rather time-consuming, we limit the effects of the environment to a finite region or "shells" surrounding the cluster. We confirm that this primitive method gives the same converged result as that obtained by the standard Ewald method.[11] In Fig. 2(a), we show the shells for the one-tetramer case, which are collections of the environmental unit cells. The central shaded unit cell is the cluster containing one tetramer and two P atoms. This is one segment of the quasi-one-dimensional chain that extends along $(\mathbf{a}-\mathbf{b})$, with $\mathbf{a}$ and $\mathbf{b}$ being two Bravais vectors, and we add the shells one by one not only on the $a$-$b$ plane but also along the $c$ axis.

Figure 2(b) shows an electric potential along the chain direction, contributed by such a collection of shells. Here, the cluster center is set at the origin of the abscissa, and the shown region spans roughly one tetramer, since one tetramer is about 10 Å long along the chain direction. In this figure, the lowest solid curve is for only one shell for every direc-

tion. The other curves are for two to four shells for every direction, although they are too close to each other to distinguish. We notice a large potential bias within a tetramer; it is nearly 1 eV at a distance of about 5 Å from the origin, that is, at the boundary of the cluster. This bias is the contribution from both the surrounding counterions and EDO-TTF molecules. Although it is interesting to know which is the major component, a direct analysis based on the cluster gives a wrong answer. This is because non-neutral components are affected by the cluster boundary that is effectively shifted when we move a measuring point from the origin. We, therefore, apply the Ewald method to each component, finding the result in Fig. 2(c). From this, we estimate that the EDO-TTF molecules are responsible for about 70% of the bias, judging from the values at 5 Å. These molecules work as averaged positive charges particularly on both sides of the cluster, and contribute to the bias. Although nearly perfect convergence is attained at the four shells, as shown in Fig. 2(b), from here on we use only one shell for this cluster, considering balance between CPU time and precision.

## III. DETERMINATION OF MOLECULAR VALENCIES

Performing self-consistent calculations with the assumption of +2 as the total valency, we find valencies of 0.18 and 0.82 at the electron-rich and electron-scarce molecules, respectively. These values are close to the experimental ones of 0.2 and 0.8 estimated by a maximum entropy method,[12] and not far from those of 0.04 and 0.96 by a Raman spectroscopy.[2] We also remark that an isolated cluster without the point charges gives unrealistic values of valencies: 0.38 and 0.62, which change by as little as 0.01, even if we enlarge the basis set from the present one, 6-31G($d$), to a rather large one, 6-311+G($2d$,$p$).

This potential bias also manifests itself in a three-tetramer cluster. As three consecutive tetramers along the chain extend in the direction of (**a**-**b**), we add the shells in a way illustrated in Fig. 2(d). We denote them as ($m$,$n$), where ($m$,$n$) means $m$ shells for the $a$-$b$ plane and $n$ shells for the $c$ axis. We tried five cases, namely, (1,1), (2,1), (2,2), (3,3), and (4,4) in this notation, to find that (2,1) gives an accuracy that is sufficient for the present purpose. In fact, the potentials for (2,1) and (4,4) are plotted in Fig. 2(e), by the solid and dashed lines, respectively, and we see that the discrepancy is rather small. From here on, we employ the former case for the DFT calculations. Regarding the potential pattern itself, we clearly observe three minima at the corresponding tetramer positions in the bias potential, each minima being similar to that in Fig. 2(b). Among these, the central one has its local bias that amounts to about 0.75 eV, again at the 5 Å distance. The reduction from the previous value found for the one-tetramer case originates from the lack of nearest-neighbor tetramers treated as the point charges. The same reason also explains the lowest energy position of the central minimum, since net positive charges corresponding to the nearest-neighbor tetramers are missing there. Such unbalance among the tetramers is compensated by the system charges determined quantum mechanically. In fact, the valency pattern for this case becomes almost regular in contrast to that

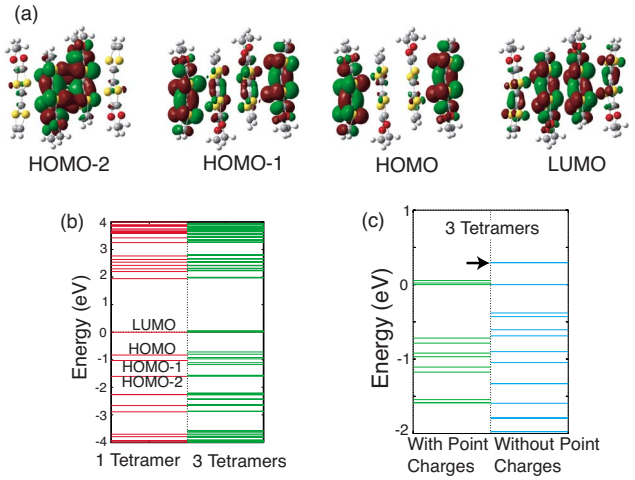


FIG. 3. (Color online) Molecular orbitals for (a) the one-tetramer cluster and [(b) and (c)] various level diagrams. In (b), the results of the point charges are shown for one tetramer and three tetramers. In (c), both are for the three tetramers, and the difference is in the existence of the point charges. In each level diagram, the energy is referenced from the LUMO level.

for the isolated case, as shown in Fig. 2(f). Moreover, we also confirm that the degree of charge disproportionation within a tetramer almost coincides with that of the one-tetramer cluster. Based on these results, we judge that our present treatment is satisfactory in spite of truncated electron itineracy beyond the cluster boundary.

## IV. NATURES OF MOLECULAR ORBITALS AND FITTING TO TIGHT-BINDING MODELS

We now proceed to more details of the calculated results. In Fig. 3(a), important molecular orbitals (MOs) are shown for the one-tetramer cluster with the self-consistent point charges. Its energy diagram also appears on the left-hand side of Fig. 3(b). As shown clearly, all these MOs originate from the same MO of an EDO-TTF molecule. The three-tetramer cluster with self-consistent point charges gives a similar MO-energy diagram as shown in Fig. 3(b). In the latter cluster, the diagram is composed of sets of almost degenerate levels, being consistent with the uniform valency pattern mentioned earlier. A small intertetramer transfer energy is considered to be the main reason for their only slightly lifted degeneracy. Meanwhile, for the three-tetramer cluster without point charges [see Fig. 3(c)], the nondegeneracy is more enhanced because of the nonuniformity among the tetramers as shown in Fig. 2(f). This feature is clearly seen for the levels originating from the lowest unoccupied molecular orbital (LUMO) of the one-tetramer case.

The energy diagram and the MOs are basically explained by the following Hückel model:

$$H = -\sum_{l\sigma} t(l)(C^{\dagger}_{l+1\sigma}C_{l\sigma} + \text{H.c.}) + \sum_{l} \Delta(l)n_l, \qquad (1)$$

where $C^{\dagger}_{l\sigma}$ ($C_{l\sigma}$) creates and annihilates an electron at the outermost MO of the $l$th EDO-TTF along an isolated chain,

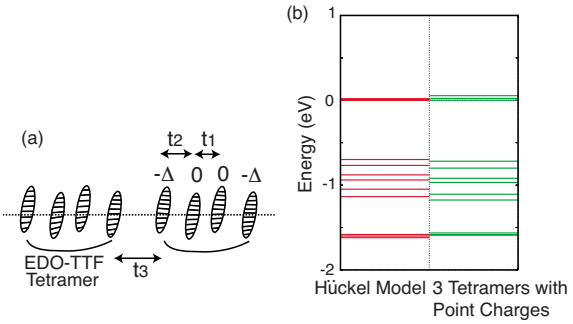


FIG. 4. (Color online) (a) Meaning of fitting parameters used for a Hückel model. (b) Comparison of two level diagrams, namely, the DFT result and a fitting by the Hückel model.

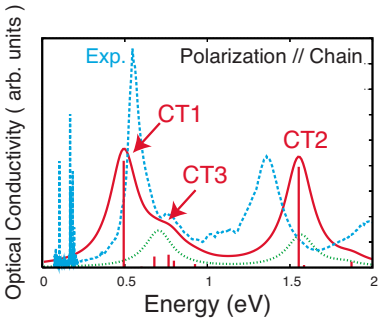


FIG. 5. (Color online) Optical conductivity spectra. The results for three tetramers and one tetramer are shown by solid and dotted lines, respectively. An experimental curve at 10 K is also shown by a dashed line. Its vertical scale is adjusted so as to give the same CT2 peak height as that of the solid line. The bars representing oscillator strengths of discrete levels are those of the three tetramers.

and $n_l$ is the number operator. It is here assumed that the effects of Coulombic interactions are included in the parameters in the mean-field sense. We first determine the values of intratetramer parameters, $t_1$ and $t_2$, and $\Delta$, as shown in Fig. 4(a), so as to reproduce the corresponding levels of the one-tetramer cluster shown in Fig. 3(b). This part of fitting is exact, since the degrees of freedom as the three relative positions of the four levels match the number of variables. After this, we add one more parameter, $t_3$, as the intertetramer transfer, and adjust it to reproduce the corresponding levels of the three-tetramer cluster shown in Fig. 3(b) as closely as possible. As a result, we obtain $t_1=0.70$ eV, $t_2=0.28$ eV, $t_3=0.17$ eV, and $\Delta=0.16$ eV. The levels thus obtained are shown on the left-hand side of Fig. 4(b). For the isolated tetramer without point charges, on the other hand, we find $t_1=0.67$ eV, $t_2=0.35$ eV, and $\Delta=-0.067$ eV. The change in $\Delta$ by more than 0.2 eV is interpreted as given by the potential bias mentioned earlier although it is effectively reduced due to spatial spreading of MOs. Another remark on the fitted values of the parameters is on the magnitude of $t_1$ relative to $t_2$. That is, the rather large $t_1$ produces energetically apart bonding and antibonding MOs of the inner molecules such as the LUMO and "HOMO-2" of Fig. 3(a). The bonding and antibonding MOs of the outer molecules then reside in between.

## V. OPTICAL CONDUCTIVITY SPECTRA

Finally, we introduce calculated results of optical conductivity spectra. In Fig. 5, we show the spectra of one tetramer and three tetramers, which are obtained by the method of the TD-DFT, with an experimental result at 10 K.[13] The self-consistent environmental point charges are also included in the calculations. The polarization here is set along the chain direction, and oscillator strengths at discrete energies are broadened with a Lorentzian width of 0.1 eV. Roughly speaking, the spectrum of the three tetramers consists of three peaks, i.e., CT1, CT2, and CT3, and reproduces the basic features of the experimental spectrum. As shown in the figure, CT1 and CT3 show almost the same energy positions as the experimental ones although CT2 is located at an energy higher than that observed. Concerning the spectral details, we first remark that the integrated oscillator strengths of CT1 and CT2 look almost the same, both in the calculation and in the measurements. Since we introduced the uniform broadening, they thus show almost the same peak heights in the calculation. In the measured spectrum, CT2 shows much larger broadening than CT1. We comment on this feature a little later.

On the basis of the MOs obtained earlier, we analyze the spectra in more detail. In the TD-DFT, each excited state is expressed as a linear combination of bare one-electron excitations although multielectron excitations are also considered implicitly in the usual sense of RPA. Inspecting principal components of each excited state, we can safely say that CT1 and CT2 have the characters of transitions from the highest occupied molecular orbital (HOMO) and HOMO-2 to the LUMO, respectively. Here, we have the MOs in Fig. 3(a) in mind. Since these transitions are optically allowed with respect to the spatial parity within a tetramer, it is natural that they appear as apparent peaks, being common to one tetramer and three tetramers. It is here emphasized that, in the spectrum of one tetramer, the two peaks correspond to CT1 and CT2, and that a feature corresponding to CT3 is absent in this case, due to the spatial parity as shown in Fig. 3(a). The above assignments of CT1 and CT2 explain their different shapes mentioned earlier, in the sense that the more localized nature of CT2 can make the width wider. Meanwhile, the peak of CT3 appears only as a weak shoulder in the measurements. In the three tetramers, the intertetramer transitions excite an electron from the "HOMO-1" orbital of a tetramer to the LUMO of its neighboring ones. Apparently, this type of transitions can be optically active, and we actually confirm this component in the ones forming CT3.

## VI. CONCLUSIONS

We have found a large electric potential bias within a tetramer of EDO-TTF molecules, namely, a building block of this material in the low-temperature phase. This is a major mechanism that explains the observed strong charge ordering. While this bias originates from long-range Coulombic interactions, it is deeply related with the internal structure of

the tetramer, i.e., the inner and outer molecules in it. As the last remark particularly related to the observed PIPT, we propose an idea that the CT2 transition will destroy most easily a tetramer structure, since it is associated with the bonding to antibonding transition in the core part of the tetramer. In fact, a drastic expansion of the distance between the two inner molecules is observed when the material undergoes thermal transition from the charge-ordered state to the metal state. Further studies to confirm this idea are now in progress and will be reported in the near future.

**ACKNOWLEDGMENTS**

The authors express their sincere gratitude for valuable experimental information including x-ray diffraction data by K. Onda, R. Tazaki, T. Ishikawa, S. Adachi, and S. Koshihara. The calculations were performed at the Research Center for Computational Science at Okazaki. This work was also supported by the Large Scale Simulation Program No. 12 (FY2006) of High Energy Accelerator Research Organization (KEK).

[1] H. Seo, C. Hotta, and H. Fukuyama, Chem. Rev. (Washington, D.C.) **104**, 5005 (2004), and references therein.
[2] O. Drozdova, K. Yakushi, K. Yamamoto, A. Ota, H. Yamochi, G. Saito, H. Tashiro, and D. B. Tanner, Phys. Rev. B **70**, 075107 (2004).
[3] K. Iwano (unpublished).
[4] M. Chollet, L. Guerin, N. Uchida, S. Fukaya, H. Shimoda, T. Ishikawa, H. Yamochi, G. Saito, R. Tazaki, S. Adachi, and S. Koshihara, Science **307**, 86 (2005).
[5] K. Onda (private communication).
[6] R. E. Stratmann, G. E. Scuseria, and M. J. Frisch, J. Chem. Phys. **109**, 8218 (1998).
[7] For example, J. E. Monat, J. H. Rodriguez, and J. K. McCusker, J. Phys. Chem. A **106**, 7309 (2002).
[8] M. J. Frisch *et al.*, GAUSSIAN 03, Revision D0.01, Gaussian Inc., Wallingford, CT, 2004.
[9] A. E. Reed, R. B. Weinstock, and F. Weinhold, J. Chem. Phys. **83**, 735 (1985).
[10] R. Chiba, H. Hiraki, T. Takahashi, X. Shao, H. Yamochi, and G. Saito, Proc. Phys. Soc. Jpn. **61**, 700 (2006).
[11] J. M. Ziman, *Principles of the Theory of Solids*, 2nd ed. (Cambridge University Press, Cambridge, England, 1972).
[12] S. Aoyagi, K. Kato, A. Ota, H. Yamochi, G. Saito, H. Suematsu, M. Sakata, and M. Takata, Angew. Chem., Int. Ed. **43**, 3670 (2004).
[13] T. Ishikawa, K. Onda, and S. Koshihara (unpublished).